

# Design and Simulation of AC to DC Low Voltage Energy Harvesting Converters

Honey Susan Eldo, Dhayalini.K

**Abstract** — In this paper, an ac/dc converter is presented that can boost very low ac voltages to a higher dc voltage. The converter is based on a new hybrid form of boost converter and a buck boost converter and it is suitable for power harvesting applications too. The measured prototype can supply 3.3V by converting an input voltage of 400mV delivered by an electromagnetic microgenerator. Detailed analysis of converter is carried out. Further; the converter is simulated with both PI control and Fuzzy control. Control algorithm using fuzzy control is described in detail. Using the simulated output waveform, comparison between PI and Fuzzy is done.

**Index Terms** — Boost converter, Buck-boost converter, PI controller, Fuzzy Logic Control.

## 1 INTRODUCTION

Energy from ambient sources are a viable alternative for supplying power to a variety of applications. Ambient energy is energy that is in the environment of the system and is not stored explicitly. Portable systems that depend on batteries have a limited operating life and can fail at inconvenient times, while a circuit powered by ambient sources has a potentially infinite life time. Inertial microgenerators which harvest mechanical energy from ambient vibrations are currently the focus of many research groups. Electromagnetic microgenerators among the various inertial generators [15] (piezoelectric, electrostatic and electromagnetic) have the highest energy density and it is considered for further study.

In electromagnetic microgenerators, small amplitude ambient mechanical vibrations are amplified into larger amplitude translational movements and the mechanical energy of the motion is converted to electrical energy by electromagnetic coupling. The output thus produced is of ac type with very low magnitude. In order to use this voltage as a supply source to electronic loads, it has to be converted into dc and must be stepped up. This requires two stages of conversion: first, ac should be rectified to dc and then it must be stepped up to the necessary dc voltage. For very low voltage as in microgenerators, rectification is not feasible by the use of conventional diodes. Even if the diode bridge rectification is possible, the forward voltage drop in diodes will cause a large amount of losses and makes the power conversion inefficient.

In this paper a new method is introduced in which low voltage ac is stepped up into dc in a single stage. A boost and a buck boost converter are connected in parallel to get the desired output.

## 2 PROPOSED CIRCUIT

The proposed circuit diagram is shown in Fig.1. It consists of a boost converter connected in parallel to a buck boost converter. Inductor L1, switch S1, and diode D1 together form the boost converter. Inductor L2, switch S2, diode D2 belongs to buck boost converter. The output capacitor C is charged by the boost converter in the positive half cycle, and by the buck boost converter in the negative half cycle. The operation of the circuit is based on the switching ON and switching OFF of both the above mentioned switches.

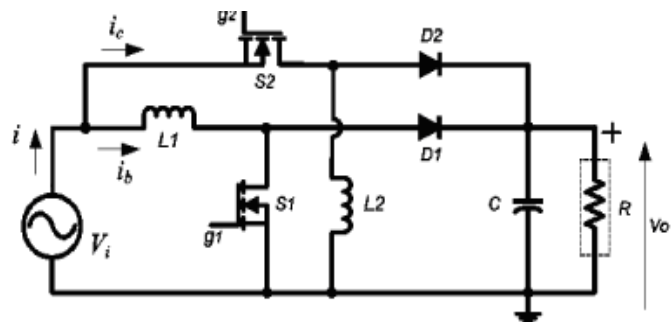


Fig. 1 Circuit diagram of ac-dc converter.

It can be noted that the input current and inductor S1 are same during both switching ON and OFF of the switch S1. But in case of buck boost converter the input current becomes zero when S2 is OFF. In order to convert and step up ac to dc, the reverse polarity of buck boost converter is used to boost the voltage of negative half cycle of microgenerator to positive dc voltage

## 3 OPERATION OF PROPOSED CONVERTER

The operation of circuit can be broadly be divided into 4 different modes. Mode 1 and 2 belongs to the positive half cycle when boost converter operates. Modes 3 and 4 belong to the negative half cycle when buck boost converter operates. During mode 1, S1 will be ON. The ac source voltage delivers power to the inductor L1, and it stores energy. In

- Honey Susan Eldo is currently pursuing her masters degree program in Power Electronics and Drives at Anna University, Chennai, India. E-mail: honeyysusaneldo@gmail.com
- Dhayalini.K is currently pursuing her PhD degree in Electrical and Electronics Engineering at Anna University, Chennai, India. E-mail: dha-ya2k@gmail.com

this mode diode D1 is reverse biased. The precharged capacitor delivers power to the load at this mode. At mode 2, S1 will be OFF. Now D1 becomes forward biased. The supply along with the energy stored in the inductor (during mode1) delivers power to the load and charges the capacitor.

During mode 3, S2 will be ON and inductor stores energy. At mode 4, when S2 is OFF, energy in L2 feeds the capacitor and the load. In a switching cycle the energy transferred to the output by a buck boost converter is equal to the energy stored in the inductor L2, whereas in the boost converter, the energy transferred to the output is more than the energy stored in the inductor. The proposed converter is operated under discontinuous mode of operation (DCM). This reduces the switch turn ON and turn OFF losses. The DCM operation also reduces the diode reverse recovery losses of the boost and buck-boost converter diodes. Furthermore, the DCM operation enables easy implementation of the control scheme. It can be noted that under constant duty cycle DCM operation, the input current is proportional to the input voltage at every switching cycle; therefore, the overall input current will be in-phase with microgenerator output voltage.

#### 4 ANALYSIS OF PROPOSED MODEL

Consider any  $k$ th switching cycle of boost and buck boost converter as shown in Fig.2.[2].  $T_s$  is the time period of switching cycle,  $D_b$  is the duty cycle of boost converter,  $d_f T_s$  is the boost inductor current fall time (diode D1 conduction time),  $D_c$  is the duty cycle of buck boost converter,  $V_i$  is the input voltage of generator with amplitude  $V_p$  and  $V_o$  is the converter output voltage. Assume switching time period ( $T_s$ ) of converter as much smaller than the time period of output ac cycle ( $T_i$ )

$$T_s \ll T_i$$

Peak value of inductor current can be obtained as

$$i_{pk} = m_1 D_b T_s = \frac{v_{ik} D_b T_s}{L_1} \quad (1)$$

$$\text{Where } v_{ik} = V_p \sin\left(\frac{2\pi k T_s}{T_i}\right)$$

After the boost converter switch is turned OFF, the current in the inductor starts to fall (see Fig. 2). The slope ( $m_2$ ) of this current is decided by the voltage across the inductor. In a  $k$ th switching cycle, the voltage across the inductor during the inductor current fall time is:  $V_o - v_{ik}$ . Therefore, the inductor current fall time can be found as in

$$d_f T_s = \frac{i_{pk}}{m_2} = \frac{i_{pk} L_1}{V_o - v_{ik}} \quad (2)$$

During this  $k$ th switching cycle, the total energy ( $E_{kb}$ ) transferred from the input of the boost converter can be obtained as in (3)

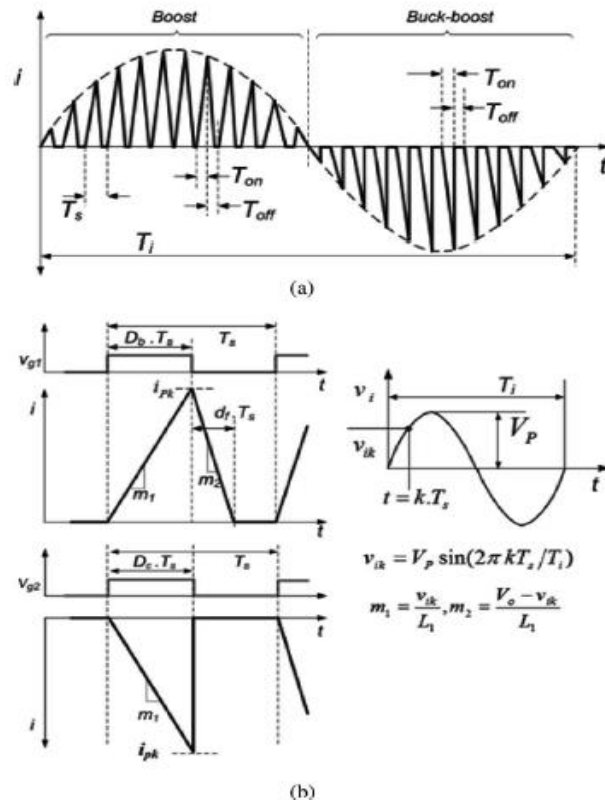


Fig.2: (a) Input current waveform of converter (b) Input currents, gate drive signals and input voltage during a switching cycle of boost and buck boost converter

$$E_{kb} = \frac{v_{ik} i_{pk} (D_b + d_f)}{2} T_s \quad (3)$$

The average power supplied in the boost switching cycle is

$$P_{kb} = \frac{E_{kb}}{T_s} = \frac{v_{ik} i_{pk} (D_b + d_f)}{2} \quad (4)$$

The number of switching cycles during the time period of one input ac cycle is defined as  $N = T_i/T_s$ . In the proposed power electronics converter topology, the boost converter is operated for the half time period of the input ac cycle ( $T_i/2$ ).

The average input power  $P_{ib}$  of the boost converter over this half cycle time period can be obtained as in (5)

$$P_{ib} = \left( \frac{2}{N} \right) \sum_{k=1}^{N/2} \frac{v_{ik} p_k (Db + df)}{2} \quad (5)$$

For large  $N$ , the discrete function in (5) can be treated as a continuous function. The average input power of the boost converter  $P_{ib}$  (5) can be obtained by integrating the term in the summation over the half cycle ( $T_i/2$ ) period of the input ac voltage and then taking its mean value. The average power of the boost converter expressed in the integration form can be obtained as in (6)

$$P_{ib} = \frac{2}{T_i} \int_0^{T_i/2} \frac{Db^2 T_s}{2L_1} V_p^2 \sin^2 \left( \frac{2\pi t}{T_i} \right) \times V_0 \left( V_0 - V_p \sin \left( \frac{2\pi t}{T_i} \right) \right)^{-1} dt \quad (6)$$

Where the microgenerator input voltage is defined as:  $v_i = V_p \sin(2\pi t/T)$ . [2]. Simplifying (6), the average input power for the boost converter  $P_{ib}$  is found to be as follows

$$P_{ib} = \frac{V_p^2 Db^2 T_s}{4L_1} \beta$$

Where

$$\beta = \left( \frac{2}{\Pi} \right) \int_0^{\Pi} \frac{1}{1 - (V_p/V_0) \sin \theta} d\theta$$

$$\text{And, } \theta = \frac{2\pi t}{T_i} \quad (7)$$

It can be noted that in (7),  $\beta$  is constant for fixed values of  $V_p$  and  $V_0$ . Also, it is seen that for large switching frequency of the converter, the average power is independent of the microgenerator output voltage frequency.

In steady state, the average input power of the converter is equal to the sum of the average output power and the various converter losses. Hence, by defining the converter efficiency as  $\eta$  for a load resistance  $R$ , the input power and the output power can be balanced as in (8)

$$\frac{V_p^2 Db^2 T_s}{4L_1} \beta = \frac{V_o^2}{R} \frac{1}{\eta} \quad (8)$$

From (8), the duty cycle of the boost converter ( $Db$ ) can be obtained as

$$Db = \frac{2V_o}{V_p} \sqrt{\frac{L_1}{RT_s \eta}} \frac{1}{\beta} \quad (9)$$

Further, consider the operation of the buck-boost converter; in this case the input power is supplied only during the ON period of the switch  $S_2$  (see Fig. 2). During the OFF period of the switch  $S_2$ , the input current is zero [see Fig. 2(a)]. Hence, for any  $k$ th switching cycle, the average power supplied by the buck-boost converter  $P_{kc}$  can be obtained as

$$P_{kc} = \frac{V_{ik} i_{pk} D_c}{2} \quad (10)$$

Applying similar approach, used earlier for the boost converter, the average power can be expressed in the integration form as

$$P_{ic} = \frac{2}{T_i} \int_0^{T_i/2} \frac{Db^2 T_s}{2L_1} V_p^2 \sin^2 \left( \frac{2\pi t}{T_i} \right) dt = \frac{V_p^2 Db^2 T_s}{4L_1} \quad (11)$$

The duty cycle  $D_c$  can be obtained as in (12)

$$D_c = \frac{2V_o}{V_p} \sqrt{\frac{L_2}{RT_s \eta}} \quad (12)$$

## 5 DESIGN OF SINGLE STAGE AC TO DC CONVERTER

For a given microgenerator and a load, the input and output voltages are specified. The voltage rating of MOSFETS is decided by the output voltage of the converter. Current rating of MOSFET has to be designed by the designer. MOSFET carries maximum current at peak input voltage. Maximum current  $I_{max}$  is given as in (13)

$$I_{max} = \frac{V_p D}{L f_s} \quad (13)$$

Here  $f_s$  is the switching frequency of converter,  $L$  is the inductance of both boost and buck boost converter, and  $D$  is the duty cycle of converter ( $Db=D_c=D$ ). Another equation used to find maximum current is

$$I_{max} = \frac{4P_{in}}{V_p D} \quad (14)$$

Fig.3 shows graph between inductor current and duty cycle. Also, the graph between inductance and duty cycle is shown. Using Fig.3, MOSFET current values and duty cycle can be selected. With these values in the given equation, the inductor value,  $L$  and switching frequency  $f_s$  can be found out. Fig.4 shows the relation between the value of inductor ( $L$ ) and the duty cycle over a range of frequencies. Using

these charts and equations, the initial values

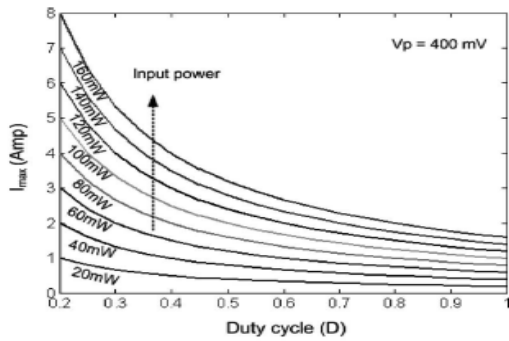


Fig.3: Design Graphs.

of the key component of the converter can be decided. The duty cycle and the frequency of the converter can be appropriately selected to choose the desired value of the inductor. In this study, the proposed converter is designed to supply about 55mW of power to the load.

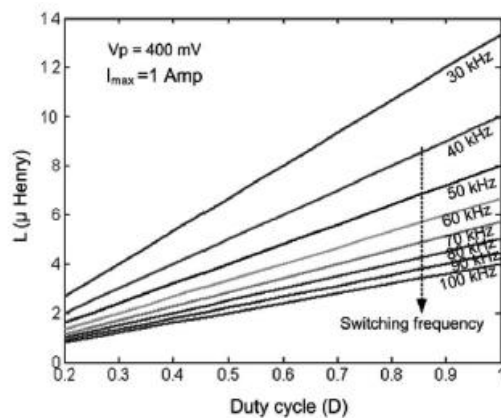


Fig.4: Design graph between inductance and duty cycle

Table 1. Circuit Components of the Converter

Circuit Components	Name	Ratings
Inductor	$L_1, L_2$	4.7uH
Inductor resistance	$R_l$	30 mΩ
N - channel MOSFET	$S_1, S_2$	20V , 2A
MOSFET on state resistance	$R_{ds, on}$	150 mΩ @ $V_{gs}=3V$
Schottky Diode	$D_1 \& D_2$	23V, 1A
Schottky Diode forward voltage	$V_f$	0.23V
Load resistance	$R$	200Ω
Capacitor	$C$	68 uF
Capacitor ESR	$R_c$	30 mΩ

## 6 FUZZY CONTROL ALGORITHM

The block diagram of the fuzzy control scheme of ac/dc converters is shown in fig.5. The fuzzy controller is divided into five modules: fuzzifier, data base, rule base, decision maker, and defuzzifier. The inputs of the fuzzy controller are the error  $e$  and the change of error  $ce$ , which are defined as

$$e = V_0 - V_{ref} \quad (15)$$

$$ce = e_k - e_{k-1}$$

where present output voltage is  $V_0$ , is the reference output voltage, and subscript  $k$  denotes values taken at the beginning of the  $k$ th switching cycle.

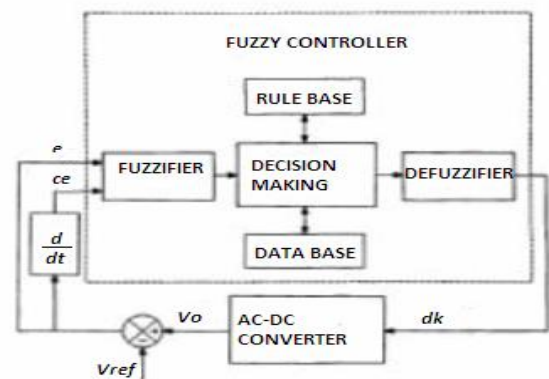


Fig.5: Block diagram of fuzzy control scheme for ac/dc converters

The output of the fuzzy controller is the duty cycle and is defined as

$$d_k = d_{k-1} + n \cdot \Delta d_{k1} \quad (16)$$

Where  $\delta d_k$  is the inferred change of duty cycle by the fuzzy controller at the  $k$ th sampling time, and  $n$  is the gain factor of the fuzzy controller. Adjusting  $n$  can change the effective gain of the controller. For ease of computation, the fuzzy variables  $e$  and  $ce$  are described by fuzzy singletons, meaning that the measured values of these variables are used in the inference process without being fuzzified. Specifically the fuzzy rules are in the form

R<sub>i</sub>: IF  $e$  is  $A_i$ ; and  $ce$  is  $B_i$ ; THEN  $d_k$  is  $C_i$

where  $A_i$  and  $B_i$  are fuzzy subsets in their universes of discourse, and  $C_i$  is a fuzzy singleton. Each universe of discourse is divided into five fuzzy subsets: PB (Positive Big), PS (Positive Small), ZE (Zero), NS (Negative Small), and NB (Negative Big). The partition of fuzzy subsets and the shape of the membership function are shown in figure 6. The values of  $e$  and  $ce$  are normalized. The triangular shape of the membership function of this arrangement presumes that for any particular input there is only one dominant fuzzy subset. Also for any combination of  $e$  and  $ce$ , a maximum of four rules are adopted. The computation time can thus be further reduced. For instance, if  $e$  is 0.1 and  $ce$  is -0.7, only (ZE, NS), (ZE, NB), (PS, NS), and (PS, NB) are in effect. The inferred grades of membership of the rest of the rules are zero.

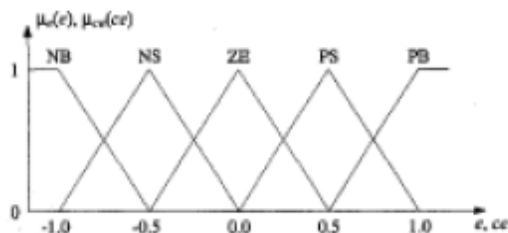


Fig.6: Membership functions for  $e$  and  $ce$

Table2. Rule Table of Fuzzy Controller

		$ce$				
		NB	NS	ZE	PS	PB
$e$	PB	-0.30	-0.35	-0.45	-0.65	-1.00
	PS	0.00	-0.10	-0.20	-0.35	-0.50
	ZE	0.20	0.10	0.00	-0.10	-0.20
	NS	0.50	0.35	0.20	0.10	0.00
	NB	1.00	0.65	0.45	0.35	0.30

The derivation of the fuzzy control rules is heuristic in nature and based on the following criteria:

- 1) When the output of the converter is far from the set point, the change of duty cycle must be large so as to bring the output to the set point quickly.
- 2) When the output of the converter is approaching the set point, a small change of duty cycle is necessary.
- 3) When the output of the converter is near the set point and is approaching it rapidly, the duty cycle must be kept constant so as to prevent overshoot.
- 4) When the set point is reached and the output is still changing, the duty cycle must be changed a little bit to prevent the output from moving away.
- 5) When the set point is reached and the output is steady, the duty cycle remains unchanged.
- 6) When the output is above the set point, the sign of the change of duty cycle must be negative, and vice versa.

According to these criteria, a rule table is derived and shown in Table II. The entries of the table are the normalized singleton values of the change of duty cycle. If the magnitude of the inferred change of duty cycle is 1, the duty cycle will be changed in full strength, which is limited by  $n$ . The inference result of each rule consists of two parts, the compatibility (weighting factor),  $w_i$  of the individual rule, and the degree of change of duty cycle,  $C_i$  according to the rule. The weighting factor  $w_i$  is obtained by applying the min operation on the  $\mu_e(e_0)$  and  $\mu_{ce}(ce_0)$  where  $e_0$  and  $ce_0$  are the singleton inputs of  $e$  and  $ce$ .  $C_i$  is looked up from the rule table II, which shows the mapping from the product space of  $e$  and  $ce$  to  $C_i$ . The inferred singleton output of each rule can therefore be written as

$$z_i = \min\{\mu_e(e_0), \mu_{ce}(ce_0)\} \quad (17)$$

$$C_i = w_i C_i$$

where  $z_i$  denotes the change of duty cycle inferred by the  $i$ th rule. After collecting all the singleton results, the next step is to defuzzify the results so that a crisp value of the change of duty cycle can be obtained. Here the method of center of gravity is preferred. The resultant change of duty cycle can be found as

$$z = \delta d_k = \frac{\sum_{i=1}^N z_i}{\sum_{i=1}^N w_i} = \frac{\sum_{i=1}^N w_i C_i}{\sum_{i=1}^N w_i} \quad (18)$$

where  $N$  is the maximum number of effective rules. In this case,  $N = 4$ . The inputs of  $e$  and  $ce$  are 0.1 and -0.7, respectively. From Fig. 6,  $e$  belongs to PS and ZE, and  $ce$  belongs to NB and NS. Thus, the four possible combinations are (1)  $e$  is PS and  $ce$  is NB; (2)  $e$  is PS and  $ce$  is NS; (3)  $e$  is ZE and  $ce$  is



NB; and (4) e is ZE and ce is NS. For each case, we calculate the weighting factor  $w$ , using the min operation, as shown in Fig. 6, and obtain the corresponding singleton value  $C$ , from the rule table. Then, the inferred change of duty cycle is computed using the above-mentioned center-of gravity method. This gives  $z = 0.086$ . The effective change of duty cycle at this sampling time is therefore  $0.086n$ .

## 7 SIMULATION OUTPUT OF CLOSED LOOP CONVERTER

A resonance-based electromagnetic microgenerator, producing 400 mV peak sinusoidal output voltages, with 100-Hz frequency is considered in this study for verification of the proposed converter topology. The reference output voltage ( $V_{ref}$ ) is considered to be 3.3 V and the switching frequency of the converter is selected to be 50 kHz. The energy-harvesting converter is designed for supplying power to a 200- $\Omega$  load resistance, hence, supplying about 55 mW of output power.

Simulation is carried out in MATLAB 7.9.0(R2009b) version. Fig 7 shows the output voltage waveform under closed loop. Under closed loop control a better output close to the desired dc voltage of about 3.267 is obtained. While in open loop a value of only 2.86V is obtained. Further, the simulation is also done under fuzzy logic control as shown in Fig.8.

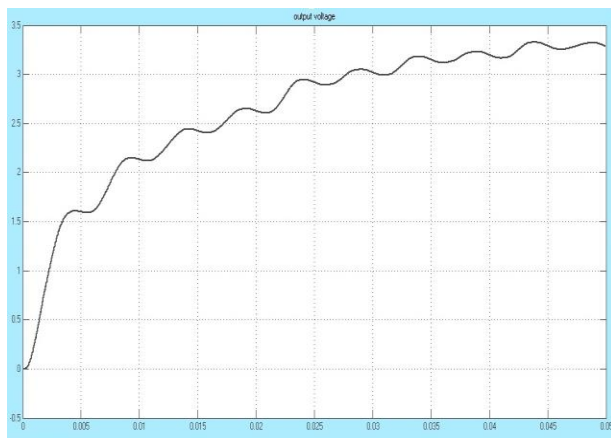
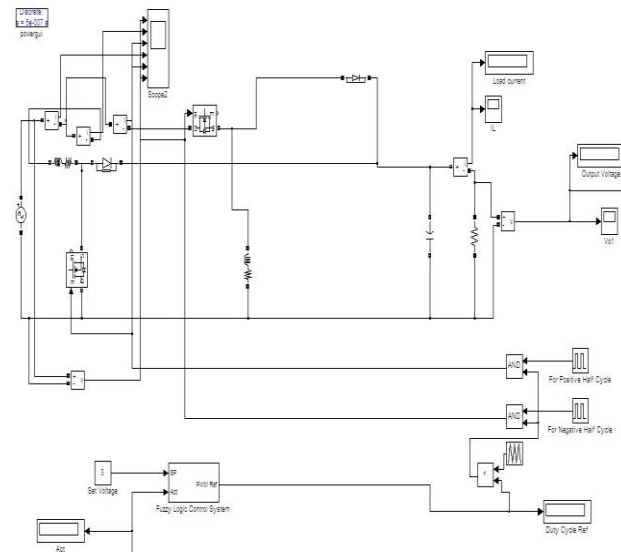


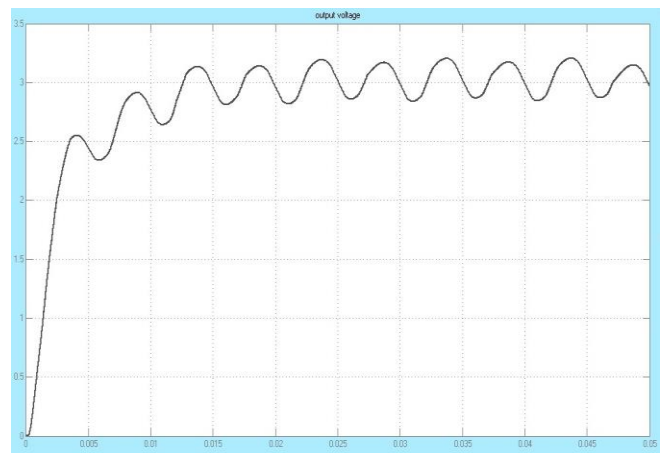
Fig.7; Output of converter with PI control

From the output voltage (Fig.8, b), it can be seen that it gives an output of about 3.3V. In spite of its practical success, fuzzy logic has been criticized for its limitations, such as the lack of a formal design methodology and the difficulty in predicting stability and robustness of FL controlled systems. The conventional control strategies have a fixed structure and fixed parameter design. Hence the tuning and optimization of these controllers is a challenging and difficult task; particularly under varying load conditions, parameter changes, abnormal modes of operation etc. Attempts to

overcome such limitations using adaptive and variable structure control have had limited success due to complexity, requiring of estimation stages model, structure changes due to discontinuous mode of operation, parameter variations, load excursions and noisy feedback. Fuzzy Logic Controller is used instead of PI to overcome the undesired overshoot coming from load impact at some abnormal conditions.



(a)



(b)

Fig.8: (a)Simulation diagram. (b) Output of converter with fuzzy control

**Table 3.Comparison of PI and Fuzzy Control**

FUZZY CONTROL	PI CONTROL
Rise time is small	takes more time to reach the target value
More flexible	Less flexible
Variation of output voltage is smaller and settles faster	Takes more time for settling
Can overcome the undesired overshoot at abnormal conditions	Overshoot coming from load impact at abnormal conditions cannot be prevented

Major disadvantages of fuzzy logic control includes

- ▶ Generally a trial and error iterative approach is taken which may be time consuming.
- ▶ Lack of a systematic procedure for design and analysis of control system.
- ▶ Lack of completeness of rule base.
- ▶ There are no definite criteria for selection of shape of membership function, and degree of overlapping of subsets.

## 9 CONCLUSION

A direct ac-to-dc low voltage energy harvesting converter is proposed in this paper. Detailed analysis of the converter for direct ac -to-dc power conversion is carried out and the relations between various converter circuit parameters and control parameters are obtained. Design guidelines are presented for selecting values of the key components and control parameters of the converter. A self-startup circuit, using a battery only during the beginning of the converter operation, is proposed for the energy-harvesting converter. Operation and the implementation of the self-startup circuit and the control circuit of the converter are presented in details.

Output of the converter in open loop, and closed loop using PI controller and fuzzy logic control are presented. Better results are obtained in closed loop circuit with fuzzy logic control.

## 10 REFERENCES

- [1] S. Meninger, J. O. Mur-Miranda, R. Amirtharajah, A. P. Chandrakasan, and J. H. Lang, "Vibration-to-electric energy conversion," *IEEE Trans. Very Large Scale Integr. Syst.*, vol. 9, no. 1, pp. 64–76, Feb. 2001
- [2] Suman Dwari and Leila Parsa, "An Efficient AC/DC Step Up Converter for Low Voltage Energy Harvesting," *IEEE Trans On Power Electronics* VOL .25,NO.8, Aug 2010.
- [3] J. C. Salmon, "Circuit topologies for single-phase voltage-doubler boost rectifiers," *IEEE Trans. Power Electron.*, vol. 8, no. 4, pp. 521–529, Oct. 1993.
- [4] S. Dwari, R. Dayal, and L. Parsa, "A novel direct AC/DC converter for efficient low voltage energy harvesting," in *Proc. IEEE Ind. Electron. Soc. Annu. Conf.*, Nov. 2008, pp. 484–488.
- [5] G. K. Ottman, H. F. Hofmann, and G. A. Lesieutre, "Optimized piezoelectric energy harvesting circuit using step-down converter in discontinuous conduction mode," *IEEE Trans. Power Electron.*, vol. 18, no. 2, pp. 696– 703, Mar. 2003.
- [7] J. Elmes, V. Gaydarzhiev, A. Mensah, K. Rustom, J. Shen, and I. Batarseh, "Maximum energy harvesting control for oscillating energy harvesting systems," in *Proc. IEEE Power Electron. Spec. Conf.*, Jun. 2007, pp. 2792–2798.
- [9] M. El-Hami, P. Glynne-Jones, N. M. White, M. Hill, S. Beeby, E. James, A. D. Brown, and J. N. Ross, "Design and fabrication of a new vibration based electromechanical power generator," *Sens. Actuators A: Phys.*, vol. 92, pp. 335–342, 2001
- [10] A. Richelli, L. Colalongo, S. Tonoli, and Z.M. Kov'acs-Vajna, "A 0.2–1.2 V DC/DC boost converter for power harvesting applications," *IEEE Trans. Power Electron.*, vol. 24, no. 6, pp. 1541–1546, Jun. 2009
- [12] K.V.Hari Prasad, CH.Uma Maheswar Rao and A.Sri Hari " Design and Simulation of a Fuzzy Logic Controller For Buck and Boost Converter" *International Journal of Advanced Technology & Engineering Research*; vol 2, Issue 3, May 2012